

# Analysis of the Quartz Crystal Resonator in Non-Electrolytic and Electrolytic Environments

Maria Isabel Osorio-Garcia<sup>1,2</sup>, Ulrike Hempel<sup>1</sup>, Ralf Lucklum<sup>1</sup>, Peter Hauptmann<sup>1</sup>.

<sup>1</sup>Institute of Micro and Sensor Systems, Otto-von-Guericke University Magdeburg, Magdeburg, Germany

<sup>2</sup>Escuela de Ingenieria de Antioquia-CES, Faculty of Biomedical Engineering, Medellin, Colombia

Email: [maria.osorio@e-technik.uni-magdeburg.de](mailto:maria.osorio@e-technik.uni-magdeburg.de)

**Abstract**—To analyze systematically the response of quartz crystal resonators (QCRs) in electrolytes, a set of experiments was performed with well controlled variations in material and experimental conditions. Three acoustic resonator configurations have been used. The sensor response in each configuration is reproducible; however, the results confirm the expected dependence of frequency shift and resistance change on the experimental setup. The extraordinary contributions to the sensor signal can be attributed to liquid conductivity and permittivity, parameters which are not considered in the common understanding of the transduction principle of QCRs. The effects measured contain useful extra information, however, the understanding of the transduction principle needs to be improved.

## I. INTRODUCTION

Kanazawa and Gordon [1] described the behavior of Quartz Crystal Resonators (QCRs) in Newtonian liquids. Their fundamental equation relates the shift in series resonant frequency (at in-phase admittance maximum),  $\Delta f_s$ , to density,  $\rho_l$ , and viscosity,  $\eta_l$ , of a liquid:

$$\frac{\Delta f_s}{f_0} = -\frac{1}{\pi Z_{cq}} \sqrt{\frac{\omega \rho_l \eta_l}{2}} \quad (1)$$

with  $Z_{cq}$  being the characteristic acoustic impedance of the quartz crystal and  $f_0$  being the fundamental frequency of the device. Many experiments with a large variety of pure liquids and liquid mixtures prove the validity of this equation. Nowadays QCR sensors appreciate an increasing interest as chemical and especially as biochemical sensors due to their unique sensitivity to the mass of molecular species. For this approach it is favorable if liquid properties can be assumed to be constant during measurement. Indeed, density and viscosity are sufficiently constant in many cases. It seems to be an obvious conclusion that the frequency shift can be attributed to changes in the recognition layer, which covers the QCR. Quite often the gravimetric assumption, i.e. the Sauerbrey-equation [2], is applied and the sensor signal is interpreted as mass change due to absorption or adsorption of (bio)-chemical entities. More involved data analysis also considers so-called non-gravimetric effects, mainly from viscoelastic properties of the coating or from interfacial phenomena. Electrical properties of the liquid, usually a buffer solution in

biochemical environment are not considered although it is known that the composition of the buffer may change in the course of the experiment. Several studies performed with electrolytes have shown that the QCR is sensitive to those properties [3-7]. However, one has to note that the experimental results differ significantly although the materials used are similar. Changes in frequency and resistance unexpected from theory have been attributed to immersion angle, surface roughness, electrode shape, fringing fields, conductivity of the solution, and the diffuse double layer. Other effects also not considered in commonly applied theoretical descriptions include non-uniformity of the coating, slip, compressional waves, mechanical stress, interfacial electronics [see e.g. 8]. Most of these disturbing factors can be excluded or at least minimized with a well designed experimental setup. Concerning the influence of electrical properties we have found a large grounded electrode facing the liquid under investigation and a smaller RF-electrode on the opposite side to be the most appropriate electrode configuration. On the one hand the electrode covering the entire surface which is in contact to the liquid prevents fringing fields from entering the liquid, mainly from the area where the contact stripe is. On the other hand the small opposite electrode guarantees a sufficient acoustic energy trapping in the inner part of the crystal; thus preventing damping from the O-rings which are necessary for sealing purposes [9]. Finally a grounded electrode prevents RF-currents leaking into the liquid (the measurement cell, pumps e.t.c. are usually grounded somewhere).

Here we analyze systematically the response of the QCR's to electrolytes. A set of experiments was performed with well controlled variations in material and experimental conditions. Three acoustic resonator configurations have been used: our traditional design with a pair of electrodes with different diameters, where the larger grounded electrode faces the liquid, the same crystal upside down with the smaller electrode grounded and a crystal without electrodes. All configurations have been exposed to three different liquids: deionized water, a set of KCl-solutions and octane. The major purpose is a variation of the overall electrical conditions while keeping the acoustic conditions (almost) constant. We only consider frequency at and magnitude of in-phase admittance (conductance) maximum, i.e., resonance frequency of the motional arm of the BVD equivalent circuit and the respective equivalent resistance.

---

This research was founded by the project ALFA PETRA II-0343-FA-FCD-FI

Although the common understanding of the BVD model does not support a dependence of this series resonant frequency on electrical properties of the liquid, namely conductivity and permittivity, we expect that the different arrangements probe the properties of the liquid in a different way. This idea is different from e.g. a previous work of Josse [10] who analyzed different electrode geometries with the purpose of optimization of the parallel resonance frequency shift. The parallel resonance frequency depends on the parallel capacitance,  $C_0$ , in the BVD model. This element is known to be the only electrical value, primarily defined by the electrode area and the quartz acting as dielectric. Fringing fields can be introduced by modification of  $C_0$  or by a separate capacitance parallel to  $C_0$ . Josse found ring-shaped electrodes to be optimal for sensing purposes. The lumped elements of the motional arm of the BVD equivalent circuit,  $L$ ,  $C$ , and  $R$  are determined by acoustically relevant properties of the sensor. They also depend on  $C_0$ ,  $C$  being proportional to  $C_0$ ,  $L$  and  $R$  being indirect proportional to  $C_0$ . Consequently  $C_0$  cancels out for the series resonant frequency, which is defined by  $L$ - $C$  product. Therefore we can expect a straightforward effect only for  $R$ . The expected influence on  $\Delta f_s$  requires a different mechanism.

## II. EXPERIMENTAL

### A. Materials

All experiments were performed with AT-cut quartz crystals resonators of 14 mm of diameter with a fundamental resonance frequency of 10 MHz. The following setups have been studied:

Setup 1: Here we use our traditional arrangement. The QCR is patterned with a pair of gold electrodes (thickness 200 nm, adhesion layer: Cr, 50 nm) with 12 and 6 mm of diameter. The large electrode was grounded and in contact with the solutions. This side is therefore called the sensing side of the crystal. The small electrode faces a reference medium, typically air, if required, dried  $N_2$ . We call this side the reference side. The contact stripe of the larger electrode goes around the edge of the crystal to allow for electrical contacts at the reference side of the crystal (Fig. 1).

Setup 2: We apply similar electrode geometry, now upside down. A pair of gold electrodes of 12 and 3 mm of diameter was exploited. The small electrode was grounded and in contact with the solutions (Fig. 2).

Setup 3: This setup employs the quartz crystal without any electrodes.

The quartz crystals employed for setup 1 and 2 were inserted into a measurement cell made of stainless steel. The cell had common ground with the SMB connector. Sealing of the liquid container was realized with O-rings having a diameter of 12 mm and a cable thickness of 1 mm. The measurement cell for setup 3 was made of polypropylene. The liquid was not grounded. We did not measure the potential, however, we assume it was afloat.

DI-water was prepared not more than 6 h before use. The resistance was  $18 \text{ M}\Omega\text{cm}^{-1}$ . KCl and octane ( $C_8H_{18}$ ) were obtained from Fluka (assay quality). Octane was employed as non-polar and non-conductive liquid. KCl solutions with concentrations ranging from 0.05 wt% to 5 wt% were prepared separately before each measurement series.

### B. Electrical setup

The quartz crystals of setup 1 and 2 have been excited in common way. The electrode-free crystal of setup 3 was driven using direct magnetic excitation. Here, a planar spiral coil of 14 mm of diameter wire thickness of 80  $\mu\text{m}$  is placed next to the crystal [11], see Fig. 3. The contact to the RF potential is located in the center of the spiral coil, whereas the connection to ground potential was at the outside. This configuration is insensitive to rotation of the QCR with respect to the spiral coil.

Measurements have been performed with a commercial network analyzer (HP4395A). The impedance spectrum of the QCR sensors with electrodes (setup 1 and 2) has been taken at 801 measurement points in a frequency range of 40 kHz including series and parallel resonance. The crystal was driven with a source power of 0 dBm. For the electrode-free crystal (setup 3) the frequency range was extended to 100 kHz and the source power increased to 15 dBm (HP4395A). The interfrequency bandwidth was 300 Hz for all arrangements. In addition, a recently in-house developed fast digital sensor-interface based on impedance analysis has been used [12]. This circuit provides higher resolution and advanced data acquisition. A graphical user interface, also developed at the institute, was used for both instruments and allowed data acquisition, processing and on-screen displaying during and after the experiments. Integrated algorithms achieve a decreased noise level in the measured spectra.

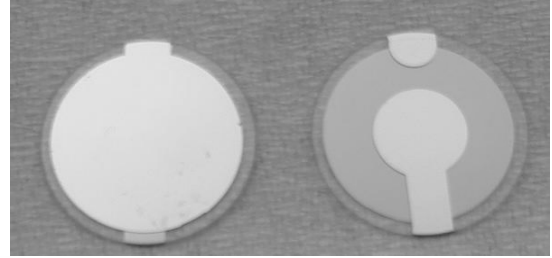


Figure 1. Quartz crystal resonator used for the standard configuration.

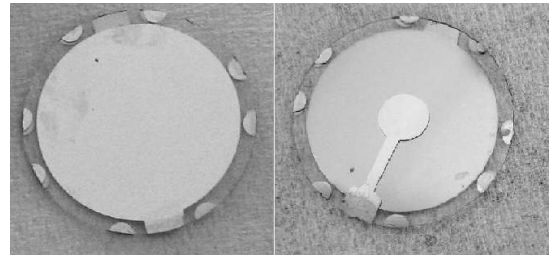


Figure 2. Quartz crystal resonator used for the upside down configuration.

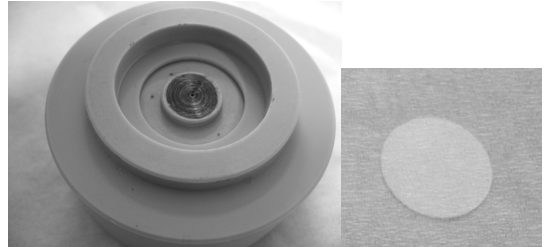


Figure 3. Quartz crystal resonator used for the planar spiral coil configuration.

### C. Procedures

The following standard procedure has been performed: Before starting the experiments, the QCRs were cleaned with potassium permanganate + sulfuric acid solution ( $\text{KMnO}_4 + \text{H}_2\text{SO}_4$ ), rinsed with DI-water and dried under nitrogen flow. The cells and all their parts were cleaned with DI water before starting the experiments. To carry out the measurements for the traditional and the upside down configuration, the complete cell was immersed in a beaker containing DI-water or the desired KCl solution. Some experiments have been performed by adding the necessary amount of KCl to DI water and sufficient long stirring to assure homogeneity of the solution, thereby gradually increasing the KCl concentration. Stirring was stopped before measurement. In all cases the immersion depth of the cell was kept constant to avoid hydrostatic pressure variations. The position of the cell was maintained as well to avoid compressional wave resonance.

Additionally, some measurements with setup 1 and 2 and all experiments with setup 3 were done by putting a 400-1000  $\mu\text{L}$  droplet of the desired solution on top of the sensing surface.

After a stable signal was reached, the frequency and the resistance were automatically determined from the impedance spectrum. All experiments were performed in a room with temperature maintained at  $22 \pm 1^\circ\text{C}$ .

### III. RESULTS AND DISCUSSION

The experiments reported here and others with similar materials and arrangements are stable, reproducible, and reveal characteristic signatures which are summarized in the following:

- Unpolar liquids applied to setup 1 are in agreement with eq. 1.
- Unpolar liquids applied to setup 2 have a 10 to 15 % larger frequency shift magnitude.
- Unpolar liquids applied to setup 3 have a frequency shift magnitude exceeding the theoretical value by 25 %.
- DI-water applied to setup 1 results in a frequency shift predicted by eq. 1.
- DI water applied to setup 2 covering only the electrode area generates a frequency shift in agreement with eq. 1.
- DI water applied to setup 2 covering the complete sensing surface produces a doubled frequency shift.
- DI water applied to setup 3 results in a frequency response increased by a factor of 2.5.
- Solutions with increasing KCl concentration increase the magnitude of frequency shift at low KCl concentrations and saturate very fast for all setups. This further decrease of the series resonance frequency is not covered by changes in the density viscosity product.
- The change in resistance is in opposite direction for setup 1 and 2. It reflects the above signatures in the respective manner.

TABLE I. COMPARISON OF FREQUENCIES AND RESISTANCES SHIFTS FOR THE DIFFERENT SOLUTIONS.

Setup	DI-H <sub>2</sub> O polar non-conductive		Octane (C <sub>8</sub> H <sub>18</sub> ) non-polar non-conductive		KCl 0.5 wt% polar conductive	
	$\Delta f$ (kHz)	$\Delta R$ ( $\Omega$ )	$\Delta f$ (kHz)	$\Delta R$ ( $\Omega$ )	$\Delta f$ (kHz)	$\Delta R$ ( $\Omega$ )
1	-1.88	114	-1.31	92	-2.24	123
2	-3.98	270	-1.48	289	-4.82	175
3	-5.41	n.a.	-1.63	n.a.	-6.31	n.a.

Representative data are summarized in Table 1. Values for the resistance could not been determined yet for setup 3 because of an unknown sensor transfer function. Figures 4-6 reflect the above statements in more detail. The average standard deviation of  $\Delta f$  in Fig. 6, 7, 8 is 12 Hz, 39 Hz, 99 Hz, respectively. The average standard deviation in Fig. 6, 7 of  $\Delta R$  is 0.6 and 0.8  $\Omega$ , respectively. The values have been determined from a set of measurements within one series. It is not surprising that magnetic direct generation exhibits the largest standard variation. The mechanical resonance is less pronounced in the impedance plot of the spiral coil; hence the series resonance frequency reading is more disturbed by noise. We also have to recognize systematic errors of unknown origin which vary from one to another measurement series. These errors, however, do not question the general statements above.

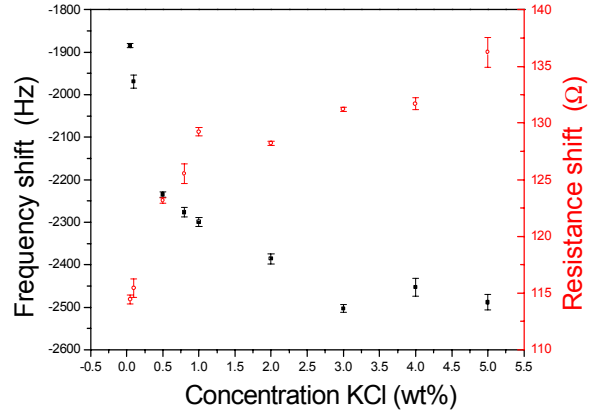


Figure 4. Experimental results for the standard setup 1. Series resonant frequency (•) and resistance shift (○) vs. concentration of KCl.

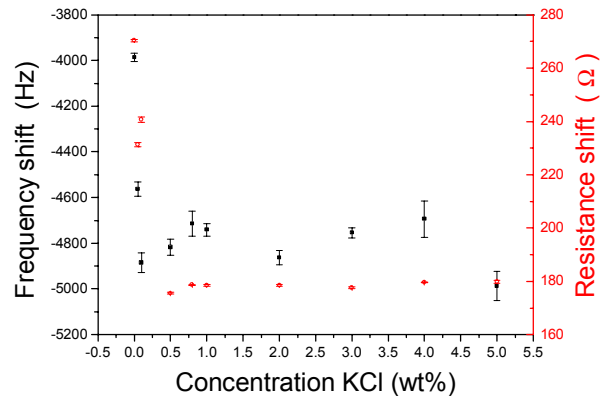


Figure 5. Experimental results for the upside down setup 2. Series resonant frequency (•) and resistance shift (○) vs. concentration of KCl.

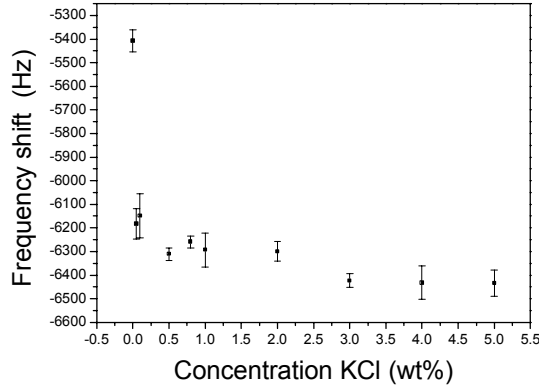


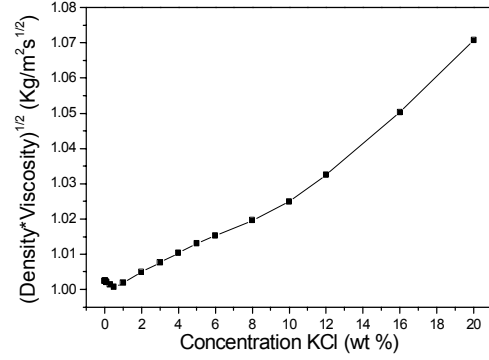
Figure 6. Experimental results for the spiral coil setup 3. Series resonance frequency shift vs. concentration of KCl.

The drop in frequency or change in resistance with KCl concentration is more pronounced for setup 2 and 3; the change with increasing KCl concentration is smoother for the traditional electrode configuration, thus setup 1 provides an extended input span for concentration measurements.

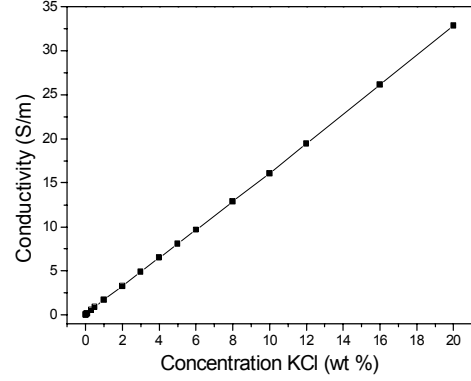
The discussion of the results requires consideration of the mechanical properties density and viscosity as well as electrical properties permittivity and conductivity. In case of the applied electrolytic solutions, all parameters change due to a variation in concentration. The values of these parameters were obtained from literature [13,14] and their dependence on concentration has been depicted in Fig 7.

Applying eq. 1 one immediately can see that the changes in liquid density viscosity can by far not explain the measured signals. We relate them to changes in liquid conductivity and permittivity. The decrease in  $R$  for setup 2 can be adequately attributed to an increase of the effective area defining the parallel capacitance due to the rapid increase of conductivity of the liquid. Saturation is an obvious consequence. Note that the absolute value is still above the value of setup 1 although in case 1 the effective area is restricted by the smaller electrode facing air and hence smaller than assumed for case 2. We conclude that although two large conductive areas face each other acoustic energy is still trapped sufficiently under the small electrode due to the non-uniform mass distribution. Fig. 8 shows a sketch of the vibration amplitude distribution. The acoustic excited area has a characteristic Gaussian distribution which is described elsewhere [15]. The electrode extension by the liquid is not comparable to the situation with two large metal electrodes. The remaining difference in the absolute values requires another explanation.

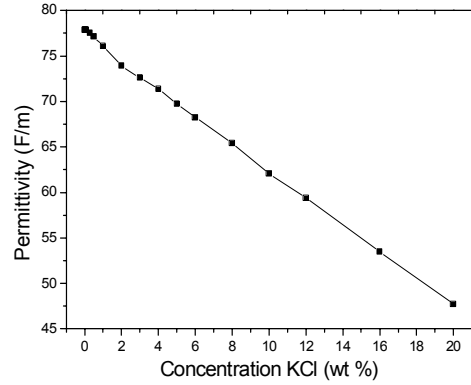
The above argumentation is also not sufficient for explaining the extraordinary frequency shift generated from an electrolyte for all setups. Due to the shielding effect of the large grounded area setup 1 the sensor should not be able to probe electrical properties of the liquid. The additional contribution of up to 500 Hz is by far too much to be explainable with a (diffuse) double layer [16] one can expect for electrochemical reasons (the measurement of the surface potential will be integrated into the setup next). The smooth surface also excludes liquid trapping.



(a)



(b)



(c)

Figure 7. Properties of the KCl solutions at different concentrations. (a) density-viscosity, (b) conductivity, (c) permittivity. Data have been taken from [13,14].

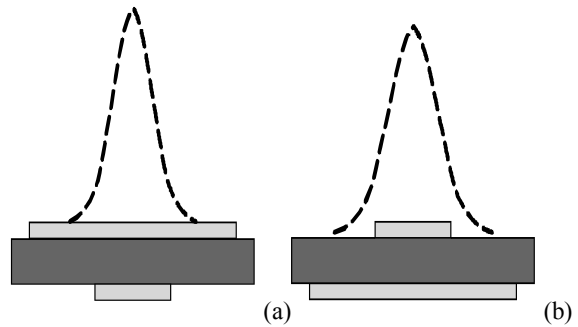


Figure 8. Sketches of the displacement distribution for QCR in contact to KCl solutions. Setup 1(a) and 2 (b).

An interfacial layer exhibiting a complex viscosity at the applied high frequency, i.e. acoustic energy storage at the interface, could provide a sufficiently large frequency shift at thicknesses around 10..20 nm, however, such an assumption is not supported by other data.

The change from DI water to an electrolyte provides an even higher (doubled) additional frequency shift when using setup 2 and 3 compared to setup 1. By contrast, here the electrical field penetrates into the liquid and probes the electrical properties. However, the mechanism, how the series resonance frequency gets affected remains unclear.

We deploy the thesis that electrically and acoustically active area may not be the same if working with electrolytes. This and the above theses require further examination.

For the spiral coil configuration the excitation mechanism is different [17]. In air the fundamental excitation of a quartz disc is achieved by the planar coil acting as an antenna and the generated electromagnetic wave coupling into the piezoelectric material. The electric field component is in plane with the resonator. A vertical electric displacement component appears due to the tensor nature of the piezoelectric permittivity. This vertical component is then the cause of the reverse piezoelectric effect creating a shear mode vibration. The second mechanism is emphasized during liquid phase measurements. Hereby, the electromagnetic resonance strength decreases strongly and a second resonance peak is enhanced. The electric potential distribution of the coil and the virtual potential of the upper face of the quartz create an electrode setup similar to the traditional excitation with one difference being the potential gradient of the coil compared to a constant potential of an electrode. Mechanical displacement is therefore also most pronounced in the center of the disc. The second difference is an electrical potential at the opposite sensing surface depending strongly on the electrical properties of the liquid and experimental conditions.

Both excitation mechanisms reveal resonance frequencies separated by several kHz due to different acoustic wave velocities. Qualitatively speaking, the effect generated due to water or electrolyte contact on the sensing side of the crystal changes the excitation mechanism of the quartz crystal and hence the resonance frequency. Indeed, putting a grounded electrode into the DI water droplet decreases the frequency by several kHz more with respect to the value shown in Fig. 6.

#### IV. CONCLUSIONS

In this work the behavior of the QCR in presence of electrolytes with three different setups is studied. Measurements of non-polar octane with all three setups showed a good agreement with commonly applied theories, that both series resonant frequency shift and change of equivalent resistance are governed by the density viscosity product of the liquid. The experiments thereby proofed the proper design of the measurement setup. Unwanted influences from surface roughness, compressional wave resonance, interface electronics e.t.c. could be excluded.

However, the experiments point out that several other material parameters of the liquid must be considered when using the QCR in polar or ionic liquids, especially the

electrical properties of electrolytes, e.g. buffer solutions. Changes in the composition may be accompanied by changes in conductivity or permittivity, which can contribute to the sensor response in an unwanted and unknown way, especially at low concentrations of salts.

The results showed that the series resonant frequency and the equivalent resistance are influenced by the specific experimental setup, especially electrode configuration and QCR excitation. In agreement with other authors the results can be attributed to liquid conductivity and permittivity of electrolytic solution such as KCl, whereas density viscosity can be excluded, since the variation of these parameters is too small. Whereas common theoretical models provide a possible transduction scheme for the response of the resistance of classical QCR sensors via changes in the active area and therefore the parallel capacitance, the transduction scheme to realize the extraordinary frequency response needs further systematic analysis.

#### REFERENCES

- [1] K.K. Kanazawa, J.G. Gordon, "Frequency of a quartz microbalance in contact with liquid," *Anal. Chem.* vol. 57, 1985 pp. 1770-1771.
- [2] G. Sauerbrey, *Z. Phys.* 1959, 155, 206.
- [3] Z.A. Shana, F. Josse, "Quartz crystal resonators as sensors in liquids using the acoustoelectric effect," *Anal. Chem.* vol. 66, 1994, pp. 1955-1964.
- [4] S. Ghafouri, M. Thompson, "Electrode modification and the response of the acoustic shear wave device operating in liquids," *Analyst*, vol. 126, 2001, pp. 2159-2167.
- [5] A. C. De Paula, M. Ferrari, D. M. Soares, V. Ferrari, "Modelling and experiments on a quartz crystal resonator sensor for conductivity measurements of low concentration ionic solutions," *Sensors & Transducers Journal*, vol. 71, 2006, pp. 711-720.
- [6] P.J. Lamas-Ardisana, A. Costa-Garcia, "Behaviour of the series resonant frequency in electrolyte solutions," *Sensors and Actuators B* vol. 115, 2006, pp. 567-574.
- [7] M. Yoshimoto, S. Tokimura, S. Kurosawa, "Characteristics of a series resonant-frequency shift of a quartz crystal Microbalance in electrolyte solutions," *Analyst*, vol. 131, 2006, pp. 1175-1182.
- [8] R. Lucklum, P. Hauptmann, R.W. Cernosek, "Thin film material properties analysis with quartz crystal resonators," 2001 IEEE Intern. Frequency Control Symp., Proc., pp. 542-550.
- [9] R. Borngräber, J. Schröder, R. Lucklum, P. Hauptmann, "Is an oscillator-based measurement adequate in a liquid environment?," *IEEE Trans. Ultrason., Ferroelec., Freq. Control* vol 49, 2002, pp. 1254 - 1259.
- [10] F. Josse, "Acoustic wave liquid-phase-based microsensors," *Sensors Actuators* vol. A 44, 1994, pp. 199-208.
- [11] F. Lucklum, P. Hauptmann, N.F. de Rooij, "Magnetic direct generation of acoustic resonances in silicon membranes," *Meas. Sci. Technol.* vol. 17, 2006, pp. 719-726.
- [12] J. Schröder, S. Doerner, T. Schneider, P. Hauptmann, "Analogue and digital sensor interfaces for impedance spectroscopy," *Meas. Sci. Technol.* vol. 15, 2004, pp. 1271-1278.
- [13] *Handbook of Chemistry and Physics*, 84<sup>th</sup> ed., CRC Press, D.R. Lide, 2003-2004
- [14] *Viscosity of pure organic liquids and binary liquid mixtures, group IV physical chemistry*, vol 18, Landolt-Börnstei.
- [15] B.A. Martin, H.E. Hager, "Velocity profile on quartz crystals oscillating in liquids," *Journal Applied Physics*, vol. 65, 1989, pp. 2630-2635.
- [16] S. Shakour Ghafouri, M. Thompson, "Interfacial properties and the response of the transverse acoustic wave device in electrolyte," *Electroanalysis*, vol. 12, 2000, pp. 326-336.
- [17] F. Lucklum, "Magnetic direct generation of acoustic resonances," Diploma Thesis, Otto-von-Guericke University Magdeburg, November 2005.